Supporting Information

Comparative Analysis of Antibodies and Heavily Glycosylated Macromolecular Immune Complexes by Size-Exclusion Chromatography Multi-Angle Light Scattering, Native Charge-Detection Mass Spectrometry, and Mass Photometry

Maurits A. den Boer[1,2], Szu-Hsueh Lai[1,2], Xiaoguang Xue[3], Muriel D. van Kampen[3], Boris Bleijlevens[3], Albert J. R. Heck[1,2,*]

[1] *Biomolecular Mass Spectrometry and Proteomics, Bijvoet Center for Biomolecular Research and Utrecht Institute of Pharmaceutical Sciences, Utrecht University, Padualaan 8, 3584 CH Utrecht, The Netherlands*

[2] *Netherlands Proteomics Center, Padualaan 8, 3584 CH Utrecht, The Netherlands*

[3] *Genmab, Uppsalalaan 15, 3584 CT Utrecht, The Netherlands*

[*] *to whom correspondence should be addressed (a.j.r.heck@uu.nl)*

Contents

Supplementary Methods

Protein samples

Anti-EGFR antibodies (2F8 mAb in IgG4Δhinge, IgG1 and IgG1-RGY format) and sEGFR were recombinantly expressed and purified by Genmab as described previously[1-4]. Purified human C1q was obtained from Complement Technology. All chemicals used were of analytical grade or higher. Protein samples were buffer exchanged to the appropriate buffer solution (150 mM ammonium acetate pH 7.5 or PBS pH 7.4) in six consecutive dilution and concentration steps at 4 °C using Amicon Ultra centrifugal filters with a 10 kDa molecular weight cutoff (Merck). Concentrations of the initial stock solutions were determined using the absorbance at 280 nm as measured by a NanoDrop 1000 spectrophotometer (NanoDrop Technologies) and the molar extinction coefficient calculated by Expasy's ProtParam. Protein complexes were assembled by mixing subcomponents at the desired molar ratios, followed by incubation at room temperature for at least 30 minutes. Anti-EGFR mAbs were incubated at 2 µM with 5 µM (MP and native MS) or 8 µM (SEC-MALS) sEGFR and/or 0.5 µM C1q. For quantitative experiments, the incubation step after preparing a dilution series was proceeded for at least 4 hours to allow re-equilibration.

Native MS

Native MS experiments were performed measuring the proteins in 150 mM aqueous ammonium acetate pH 7.5. Samples were loaded into gold-coated borosilicate capillaries (prepared in house) for direct infusion from a static nano-electrospray ionization source. Quantitative analyses of IgG1-RGY hexamers were performed on a modified LCT time-of-flight instrument (Waters), measuring each sample of a dilution series in triplicate for 1 min (30 scans) after a stable signal had been obtained. Data were processed in MassLynx V4.1 (Waters), followed by analysis using an in-house script that sums and compares ion intensities within the *m/z* ranges that we assigned to the different species. This approach is similar to a method described by Wang et al[5]. All other experiments were performed on a Q Exactive Plus UHMR Orbitrap instrument (Thermo Fisher Scientific), typically collecting at least 100 scans. The set resolution of the instrument at *m/z* 200 was 50,000 for IgG1, 6250 for sEGFR, 25,000 for IgG1 + sEGFR, 50,000 for individual measurements of IgG1-RGY and C1q, and 25,000 for complexes of IgG1-RGY, sEGFR and C1q, Data were exported from Thermo Xcalibur Qual Browser 4.2.28.14 (Thermo Fisher Scientific), and all figures were prepared using an in-house Python script in Jupyter Notebook. Masses were determined by Bayesian deconvolution using UniDec 4.4.1[6].

Native CD-MS

Similar as for the normal native MS experiments, samples were introduced into a Q Exactive Plus UHMR Orbitrap mass spectrometer, though operated with a relatively low collision gas pressure (N_2). The pressure readout of the UHV sensor was controlled below $2 \cdot 10^{-10}$ torr. The instrumental resolution was set to 280,000 at 200 *m/z* (transient of 1 s) for accurate detection of both *m/z* and *z*. After multiscan acquisition, RAW files were centroided and converted into mzXML format, followed by filtering out ions that were dephased during the transient and therefore occurred as split peaks[7]. The intensity noise threshold was set to the level corresponding to 8 elementary charges. After the filtering, the remaining centroids of single ion events are more confined in the intensity domain as well as their charge states. In this work, a calibration factor of 12.55 (normalized arbitrary intensities/charges) was used for correlating the measured intensities and charges of individual single ions. Several mzXML files could be merged into one for providing improved statistics. According to the determined charge state, a resulting formula mass = $m/z \cdot z - z$ was used to calculate the mass of every single ion. Finally, entire mass distributions were plotted and fitted with a normal distribution in the histogram (mass and counts) with an appropriate bin size (10 kDa).

SEC-MALS

SEC-MALS data were collected using a Waters HPLC with an in-line UV detector (Waters 2487 Dual Absorbance), a MALS detector (MiniDAWN, Wyatt Technology) and an RI detector (Optilab, Wyatt Technology). Analysis was performed on an SRT SEC-500 column (Sepax Technologies) using 100 mM sodium phosphate, 100 mM sodium sulfate, pH 6.8 as mobile phase at 0.35 mL/min flow rate. By simultaneously measuring the light scattering and the concentration of the molecules as they elute from the column, the molar mass of the particle could be determined. As concentration determination by UV absorbance requires prior knowledge of the extinction coefficient, this brings SEC-MALS to a problem of circularity when the aim is to determine the stoichiometry of a complex using only a UV detector as concentration source. This problem is overcome by using a refractive index (RI) detector, which can assess concentrations directly. MALS data were processed by ASTRA software (Wyatt version 8.00.25) based on MALS-RI for antibody mass determinations (using the RI detector as concentration source with a *dn/dc* of 0.185) and with the Protein Conjugate Analysis method (MALS-UV-RI) to get information on the individual contributions of a) glycan and protein for the glycosylated proteins and b) different protein subunits for the complexes. For data processing of the individual glycosylated proteins, *dn/dc* values of 0.185 and 0.140 were used for as input for "protein" and "modifier" (glycan) portions respectively. The complexes were processed in a multi-step approach essentially according to Hastie *et al*.[8]. First, the antibody-antigen complex was analyzed using the Protein Conjugate Analysis method with the antibody assigned as "protein" and the antigen (sEGFR) as "modifier". For the antibody, a *dn/dc* of 0.185 and the UV extinction coefficient as calculated by ASTRA from MALS-RI analysis of the individual antibody were entered as "protein" parameters. For the antigen, these values were derived from MALS-UV-RI analysis of the individual compound, as calculated by ASTRA, and entered as "modifier" parameters. The three-component C1q-antibody-sEGFR complex was analyzed taking the calculated UV extinction coefficient and *dn/dc* values from the previous steps as input values. Results are reported as molar mass at the UV peak maximum (M_p).

Mass photometry

MP experiments were performed on a Refeyn One[MP] mass photometer (Refeyn), measuring all samples in PBS. Borosilicate microscope coverslips (24 x 50 mm 1.5H, Marienfeld) were cleaned in four sequential sonication rounds of 5 min using isopropanol and MilliQ water (2x). Silicone cell culture gaskets (50 wells, 3 mm diameter x 1 mm depth, Grace Bio-Labs) were cut into sets of four wells, which were placed onto clean coverslips. Before data acquisition, coverslip wells were loaded with approximately 12 µL PBS, followed by focusing the instrument on the glass-liquid interface. All samples were measured in triplicate. Typically, samples were added by pipetting 3 µL of a diluted solution directly into the PBS-loaded well to a final concentration of 1-30 nM, followed by recording for 150 s (12,000 frames). When measuring protein complexes, higher concentration solutions in the µM range were jump diluted to nM range concentrations, starting the recording within 5-30 s from the initial dilution step. Recordings were processed in DiscoverMP (Refeyn) and calibrated using an in-house calibration mix consisting of proteins of which accurate masses had previously been determined by MS (73 kDa IgG4Δhinge-L368A, 149 kDa IgG1-Campath, 483 kDa apoferritin, and 800 kDa GroEL). Data analysis and plotting were performed in Jupyter Notebook using an in-house Python library, combining multiple measurements of the same sample into a single dataset. For quantitative MP experiments, we jump diluted samples from a dilution series in triplicate and recorded for 75 s (6000 frames). Dissociation of protein complexes upon jump dilution was modelled to infer their abundance in the original solution (see below).

Modelling IgG4Δhinge dissociation to estimate the fractional occupancy before jump dilution using MP

Determining K_d values works best when the sample is analyzed at concentrations around the K_d value of the analyte, the point at which 50% is bound. MP experiments are however mostly performed at nM range concentrations, limiting the ability to assess µM-mM range affinities. This problem can be partially overcome by jump dilution just before measurement, as the distribution of protein species then roughly corresponds to the equilibrium before dilution. However, this method only works if the k_{off} is relatively low. In practice, when k_{off} is not

low, the complex can dissociate during the measurement, which needs to be corrected for. Our solution to this problem is to infer the k_{off} of the interaction from the observed decay of protein complexes over time, which can then be used to estimate the complex abundance at the instant of dilution (t = 0).

For IgG4Δhinge, the concentration of (HL)$_2$ over time can be described using the following equation:

(S1) $\quad [(HL)_2] = f(t) = \left([(HL)_2]_0 - [(HL)_2]_{eq}\right) \cdot e^{-(k_{on} \cdot [HL] + k_{off}) \cdot t} + [(HL)_2]_{eq}$

In this formula, $[(HL)_2]_0$ is the concentration of (HL)$_2$ at the instant of jump dilution, while $[(HL)_2]_{eq}$ is the equilibrium concentration under measurement conditions. However, when measuring at concentrations far below the K_d, we can assume that $[(HL)_2]_{eq}$ and $k_{on} * [HL]$ are close to zero:

(S2) $\quad [(HL)_2] = f(t) = [(HL)_2]_0 \cdot e^{-k_{off} \cdot t}$

The fractional occupancy corresponding to $[(HL)_2]_0$ is then identical to the fractional occupancy at the concentration before dilution (t=-1). Therefore:

(S3) $\quad [(HL)_2]_0 = \frac{FO_{-1} \cdot [(HL)_{total}]_0}{2}$

With:

(S4) $\quad FO = \frac{2 \cdot [(HL)_2]}{[(HL)_{total}]}$

Only $[(HL)_{total}]_{-1}$ is known. However, we can write $[(HL)_2]$ as a function of $[(HL)_{total}]$ and the K_d:

(S5) $\quad K_d = \frac{[A][B]}{[AB]} = \frac{[HL][HL]}{[(HL)_2]}$

(S6) $\quad K_d = \frac{([(HL)_{total}] - 2[(HL)_2])^2}{[(HL)_2]}$

(S7) $\quad [(HL)_2]K_d = ([(HL)_{total}] - 2[(HL)_2])^2$

(S8) $\quad [(HL)_2]K_d = [(HL)_{total}]^2 - 4[(HL)_2][(HL)_{total}] + 4[(HL)_2]^2$

(S9) $\quad 4[(HL)_2]^2 - (4[(HL)_{total}] + K_d)[(HL)_2] + [(HL)_{total}]^2 = 0$

Which has the form:

(S10) $\quad ax^2 + bx + c = 0$

According to the quadratic equation:

(S11) $\quad [(HL)_2] = \dfrac{(4[(HL)_{total}]+K_d) - \sqrt{(4[(HL)_{total}]+K_d)^2 - 16[(HL)_{total}]}}{8}$

Therefore $[(HL)_2]_0$ is:

(S12) $\quad [(HL)_2]_0 = \dfrac{FO \cdot [(HL)_{total}]_0}{2} = \dfrac{\frac{2 \cdot [(HL)_2]_{-1}}{[(HL)_{total}]_{-1}} \cdot [(HL)_{total}]_0}{2}$

(S13) $\quad [(HL)_2]_0 = \dfrac{\frac{2 \cdot \frac{\left(4[(HL)_{total}]_{-1}+K_d\right) - \sqrt{\left(4[(HL)_{total}]_{-1}+K_d\right)^2 - 16[(HL)_{total}]_{-1}}}{8}}{[(HL)_{total}]_{-1}} \cdot [(HL)_{total}]_0}{2}$

(S14) $\quad [(HL)_2]_0 = \dfrac{(4[(HL)_{total}]_{-1}+K_d) - \sqrt{(4[(HL)_{total}]_{-1}+K_d)^2 - 16[(HL)_{total}]_{-1}}}{8[(HL)_{total}]_{-1}} \cdot [(HL)_{total}]_0$

And the concentration of $(HL)_2$ over time is:

(S15) $\quad [(HL)_2] = \dfrac{(4[(HL)_{total}]_{-1}+K_d) - \sqrt{(4[(HL)_{total}]_{-1}+K_d)^2 - 16[(HL)_{total}]_{-1}}}{8[(HL)_{total}]_{-1}} \cdot [(HL)_{total}]_0 \cdot e^{-k_{off} \cdot t}$

Alternatively, we can describe FO over time:

(S16) $\quad FO = \dfrac{(4[(HL)_{total}]_{-1}+K_d) - \sqrt{(4[(HL)_{total}]_{-1}+K_d)^2 - 16[(HL)_{total}]_{-1}}}{4[(HL)_{total}]_{-1}} \cdot e^{-k_{off} \cdot t}$

The unknown k_{off} can then be estimated by fitting the above formula to the measurement of FO over time. This also gives a first indication of the K_d. However, fitting can best be done on a linear scale, which is why we used ln(FO).

(S17) $\quad \ln(FO) = \ln\left(\dfrac{(4[(HL)_{total}]_{-1}+K_d) - \sqrt{(4[(HL)_{total}]_{-1}+K_d)^2 - 16[(HL)_{total}]_{-1}}}{4[(HL)_{total}]_{-1}}\right) + \ln\left(e^{-k_{off} \cdot t}\right)$

(S18) $\quad \ln(FO) = \ln\left(\dfrac{(4[(HL)_{total}]_{-1}+K_d) - \sqrt{(4[(HL)_{total}]_{-1}+K_d)^2 - 16[(HL)_{total}]_{-1}}}{4[(HL)_{total}]_{-1}}\right) - k_{off} \cdot t$

In order to determine the k_{off}, high-concentration samples of each IgG4Δhinge variant were jump diluted and measured for 10 minutes in triplicate, pipetting the solution up and down every two minutes to keep a sufficient detection rate (**Figure S1**). For assemblies with high k_{off} values, we only considered the first 100 s of the measurement, as the decay rate of FO already started to level off as the sample approached equilibrium. Equation S18 was then fitted to the data using linear least squares regression, readily revealing k_{off} values spanning three orders of magnitude.
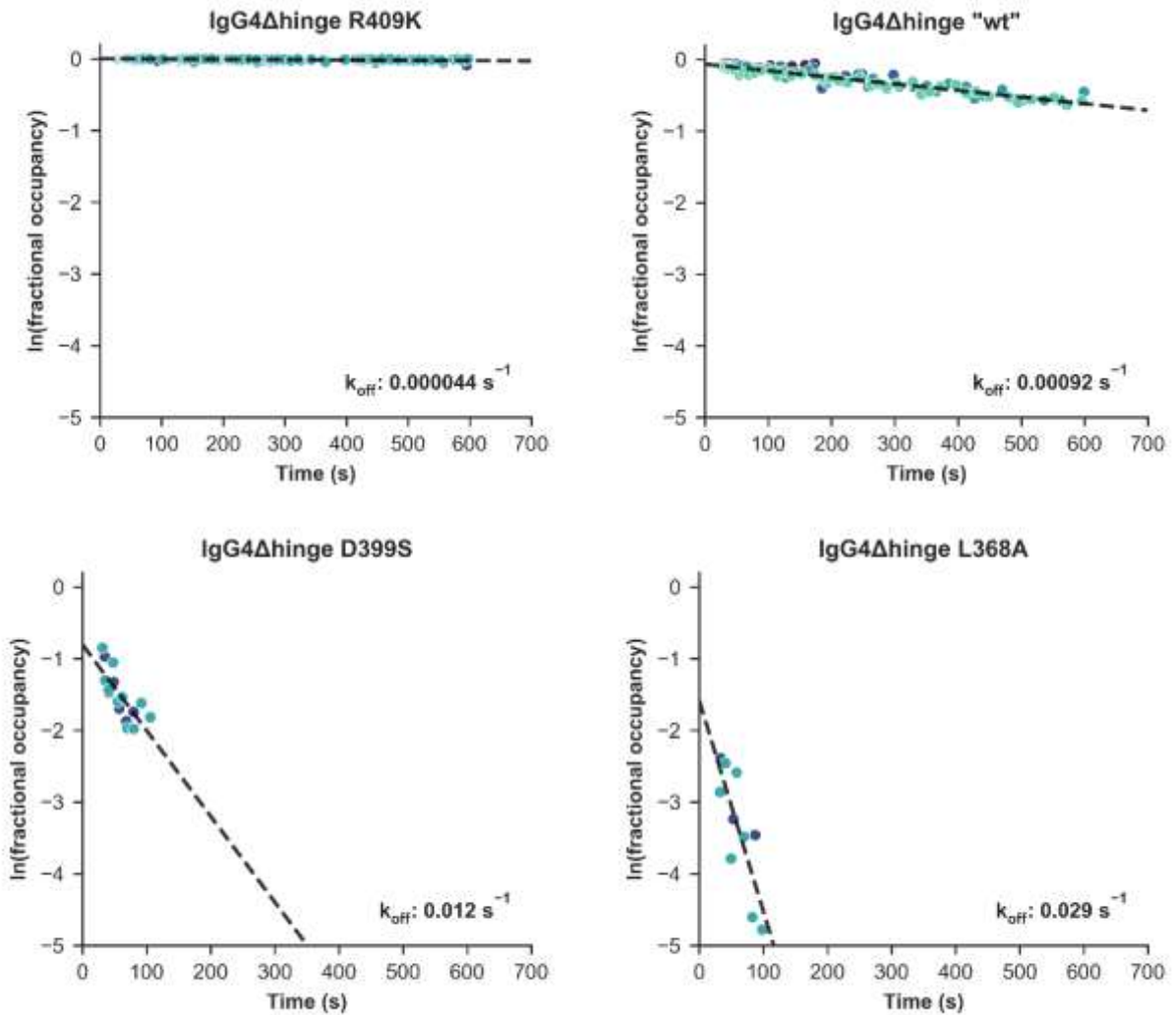
Figure S1. Using MP to determine the k_{off} of IgG4Δhinge variants by following the fractional occupancy of the dimer over time. High-concentration samples were jump diluted and measured for 10 minutes, pipetting the solution up and down every two minutes to maintain a sufficient detection rate. Events were assigned to (HL) or (HL)$_2$ based on a mass window corresponding to an equal portion of the normal distribution (e.g., from μ - 2σ to μ + 2σ). Assigned events were grouped into bins of 100, followed by calculating the fractional occupancy within the bin (colored for different replicates). Equation S18 was fitted to the data using linear least squares regression to estimate the k_{off} of the interaction (black line).

Measuring affinities by dissociation-corrected jump dilution MP

The K_d of IgG4Δhinge variants was determined by measuring a dilution series in triplicate using a standard recording length of 75 s (6000 frames). To correct for jump dilution-induced dissociation, we fitted equation S18 with the previously determined k_{off} to each measurement to in infer the fractional occupancy at t=0. Fits were checked manually, and poor fits were removed upon inspection of the original data, for example when too few binding events were available. Furthermore, because K_d determination gets increasingly inaccurate at the extremes of fractional occupancy (nearly 0% or 100% dimer), where possible, we only considered data points where 5% < FO < 95%.

Using the estimated fractional occupancy, [HL] and [(HL)$_2$] can be calculated. The ratio between these concentrations gives the K_d:

(S19) $K_d = \frac{[HL][HL]}{[(HL)_2]}$

(S20) $[HL]^2 = [(HL)_2] \cdot K_d$

In a plot of [HL]^2 versus [(HL)$_2$], the slope thus gives the K_d. However, the concentration points in the dilution series were not distributed on a linear scale, but rather a logarithmic scale. To avoid overweighting of the highest concentration points, we therefore proceeded with a log transform of the dataset:

(S21) $\log([HL]^2) = \log([(HL)_2] \cdot K_d) = \log([(HL)_2]) + \log(K_d)$

We used least squares fitting of equation S21 to the determine the overall K_d, which in a plot of log([HL]^2) versus log ([(HL)$_2$]) is defined by the intersect with the y-axis (**Figure S2**).
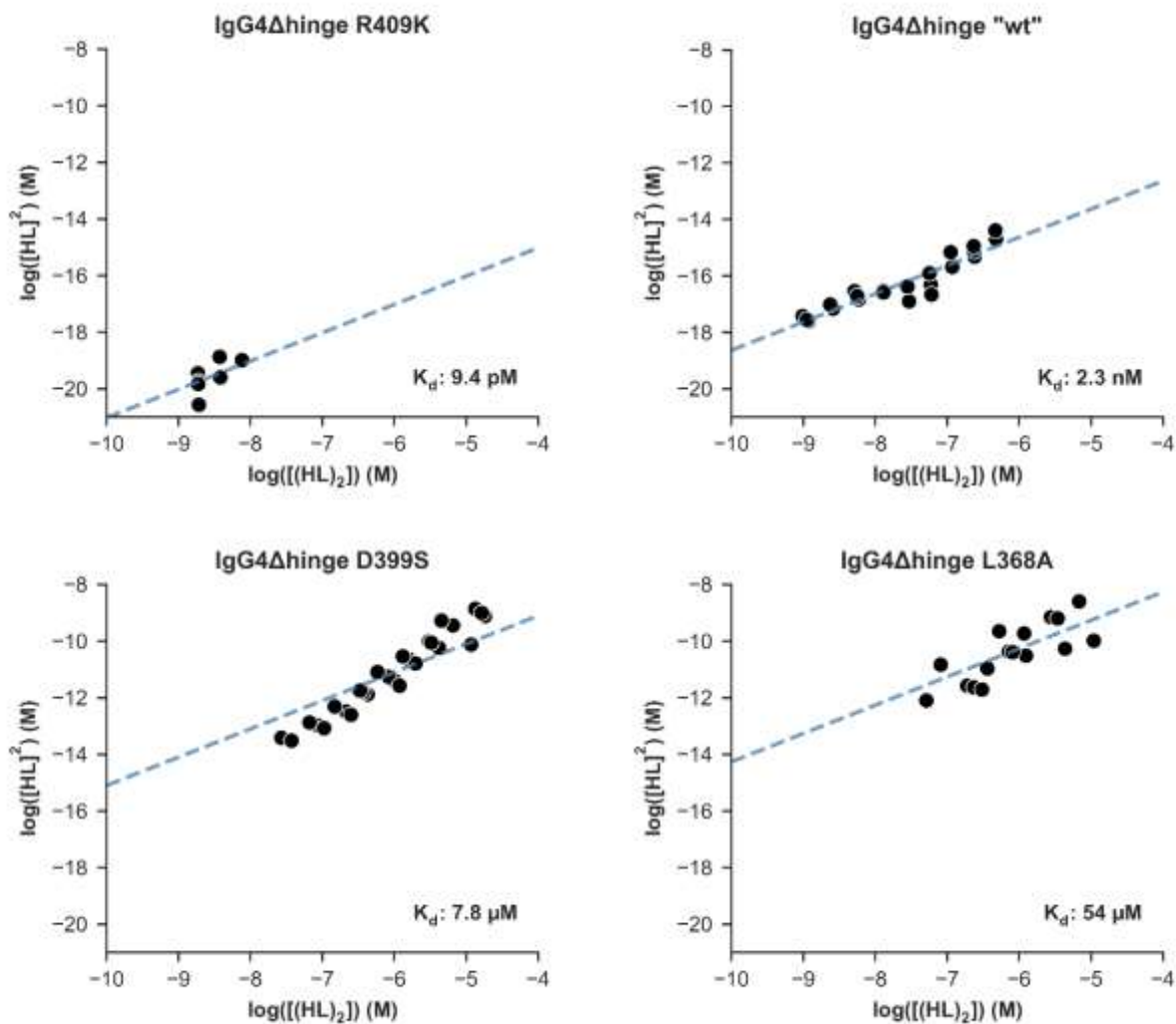
Figure S2. Assessing the K_d of IgG4Δhinge variants from a dilution series by dissociation-corrected MP. A dilution series of IgG4Δhinge variants was measured by jump dilution MP in triplicate, followed by inference of the fractional occupancy at t=0 using the previously determined k_{off}. Fits were checked manually, outliers were removed, and when possible, we only considered measurements where 5% < FO < 95%. The apparent K_d of each measurement was then determined by linear least squares fitting of equation S21 (blue line), revealing the overall K_d value.

Supplementary Figures
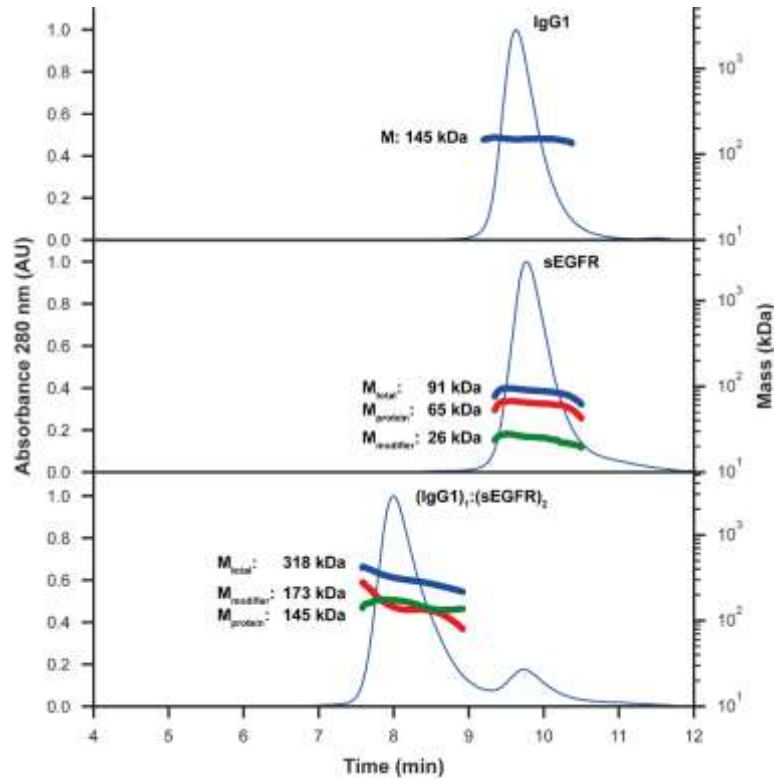
Figure S3. Characterizing highly heterogeneous antibody-antigen complexes involving IgG1 and sEGFR by SEC-MALS. Using the RI detector for direct concentration measurement, SEC-MALS quite accurately determined the mass of IgG1 anti-sEGFR. For more complex samples, SEC-MALS-UV-RI "protein-conjugate" analysis enabled disentanglement of the mass contributions of a protein backbone (based on the UV absorption coefficient) and a modifier (glycans or a binding partner) from the total mass. This approach enabled total mass determination for sEGFR, while simultaneously analyzing of the contribution the protein backbone (protein) and glycans (modifier). When 2 μM of IgG1 was incubated with 8 μM of sEGFR, similarly, the mass of the full (IgG1)$_1$:(sEGFR)$_2$ complex could be determined, disentangling the contributions from the IgG1 (protein) and two bound sEGFR molecules (modifier).
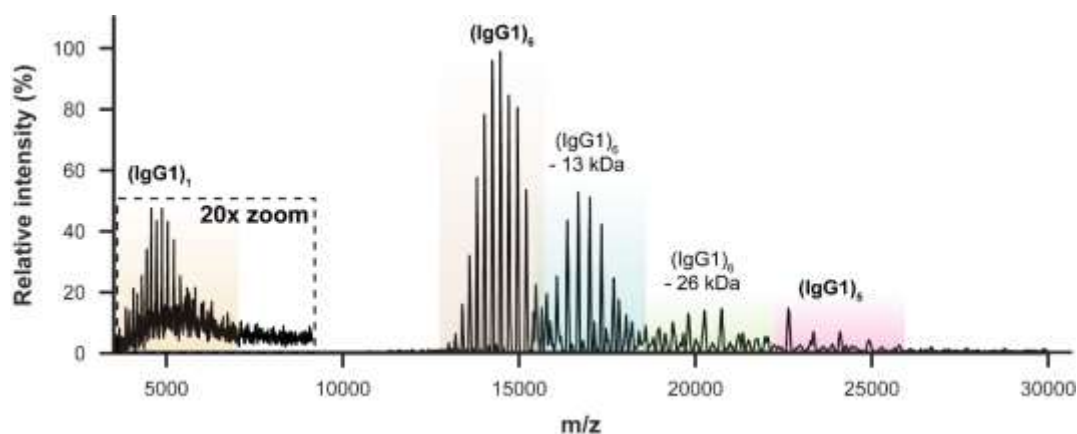
Figure S4. Gas phase activation of IgG1-RGY hexamers leads to ejection of a highly charged IgG1 monomer. The charge state envelope of (IgG1)$_6$ was isolated by the quadrupole of the instrument, followed by collisional activation using Xenon gas in the HCD cell. This led to the ejection of a highly charged monomer, concomitant with a lowly charged pentamer. We additionally observed the ejection of 13 kDa polypeptides from the hexameric complex, likely resulting from a specific backbone cleavage in the Fab portion of the antibodies.
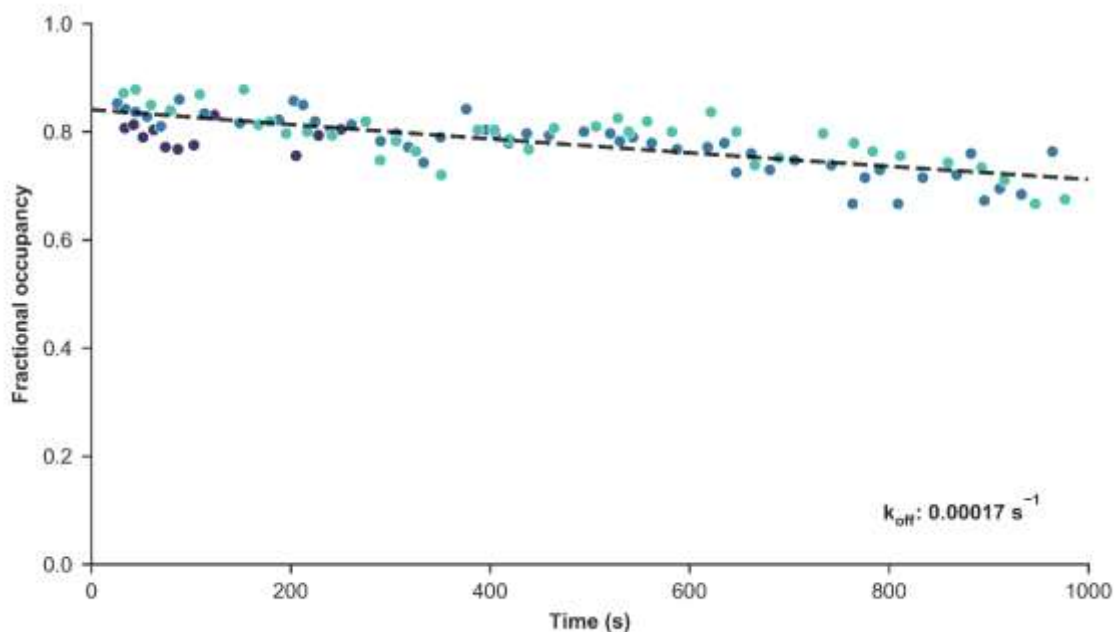
Figure S5. IgG1-RGY hexamers dissociate slowly upon jump dilution MP. IgG1-RGY samples of 8 µM were jump diluted to a measurement concentration of 10 nM, followed by a MP recording of 10 minutes, pipetting the solution up and down every two minutes to maintain a sufficient detection rate. Events were assigned to (IgG)$_1$ or (IgG)$_6$ based on a mass window corresponding to an equal portion of the normal distribution (μ - 2σ to μ + 2σ). Assigned events were grouped into bins of 100, followed by calculating the fractional occupancy within the bin (colored for three different replicates). An exponential decay function was fitted to linearized (logarithmically transformed) data using linear least squares regression to estimate the overall k_{off} of the interaction (black line).
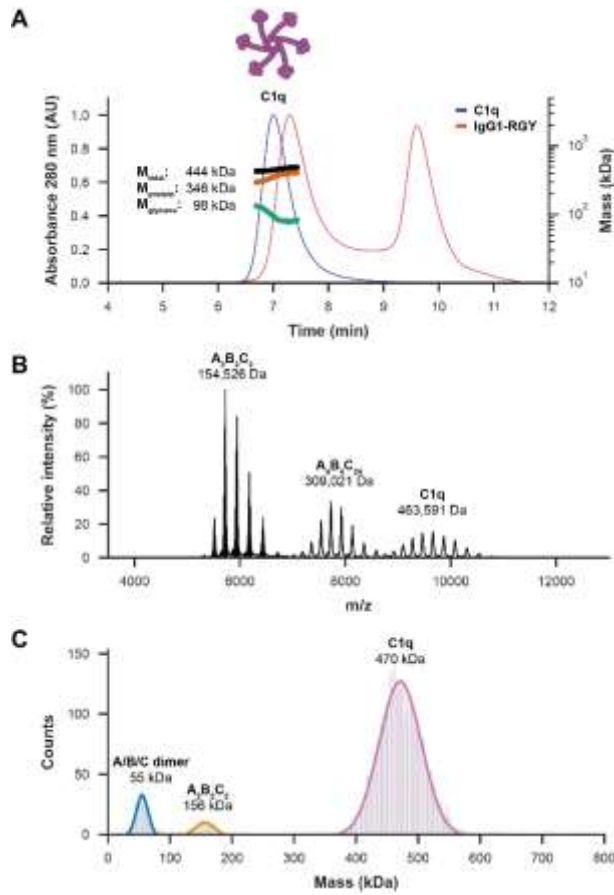
Figure S6. The complement recognition complex C1q is reliably mass analyzed by MP while analyses by native MS and SEC are hampered by technique-related artifacts. A. The SEC chromatogram of C1q reveals one elution peak at a relatively short retention time, suggesting a > 1 MDa particle, while MALS reveals a mass of 444 kDa, closely matching C1q. SEC-MALS-UV-RI analysis based on the calculated UV extinction coefficient revealed contributions of 346 kDa from the protein backbone and 98 kDa from the glycans. For comparison the chromatogram of IgG-RGY is overlayed. **B.** While native MS measures an accurate mass of 464 kDa for the intact C1q complex, it reveals the presence of 2-, 4-, and 6-armed versions of C1q. These smaller complexes likely result from dissociation induced in the source region. **C.** Characterization of C1q by MP reveals a main mass distribution of particles corresponding to the full 6-armed C1q complex with a smaller contribution being made by a 2-armed complex. Masses closely match those observed by native MS.
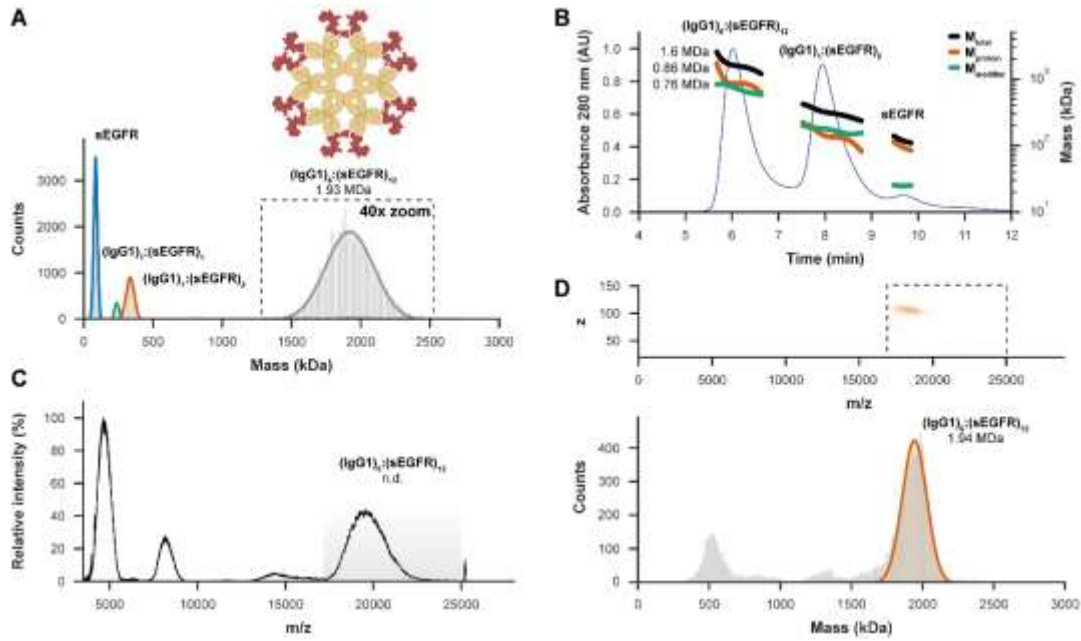
Figure S7. MP and CD-MS successfully determine the mass and full occupancy of highly heterogeneous (IgG1)₆:(sEGFR)₁₂ antibody-antigen complexes. A. MP measurements of anti-EGFR IgG1-RGY hexamers incubated with sEGFR reveal the presence of particles with an average mass of 1.93 MDa, likely corresponding to (IgG1)₆:(sEGFR)₁₂. **B.** SEC-MALS-UV-RI reveals the presence of larger immune complexes with a total estimated mass of around 1.6 MDa (~0.86 MDa for (IgG1)₆ with a ~0.76 MDa modifier, i.e., sEGFR molecules). The mass accuracy of SEC-MALS is in this case insufficient for determining the exact stoichiometry of (IgG1)₆:(sEGFR) complexes. **C.** Native mass spectra of the same sample show that although large ion species are detected at about *m/z* 20,000, they cannot be charge-resolved, preventing mass determination. **D.** Two-dimensional charge-detection MS spectra revealing the *m/z* and *z* of single ions independently, circumventing the need for charge-state resolution. For the main particle population an average mass of 1.94 MDa was determined, corresponding to the fully occupied (IgG1)₆:(sEGFR)₁₂ complex (bottom).

Supplementary Tables

Table S1. **Comparison of mass measurements of proteins and protein complexes between native MS, CD-MS, MP and SEC-MALS**. For native MS, when individual proteoglycoforms could be resolved, the intensity-weighted average mass is indicated. For MP, masses indicate the mean of a normal distribution fitted to a range of single-particle mass measurements. For CD-MS, masses indicate the maximum of a kernel density estimation. Masses measured by MP and SEC-MALS are compared to highly accurate masses determined by native MS. For complexes involving sEGFR, the expected mass was calculated from the sum of components using a previously reported tandem MS-derived mass for sEGFR[9]. These expected values are given in italics and in parentheses.

Species	$MW_{Native\ MS}$ (kDa)	MW_{CD-MS} (kDa)	ΔMW_{CD-MS} (%)	MW_{MP} (kDa)	ΔMW_{MP} (%)	$MW_{SEC-MALS}$ (kDa)	$\Delta MW_{SEC-MALS}$ (%)
IgG4Δhinge HL	73.196			74	1.1%	-	-
IgG4Δhinge (HL)$_2$	146.358			146	-0.2%	-	-
sEGFR	*(87.5)*	87.7	0.2%	86	-1.7%	91	4.0%
IgG1 anti-sEGFR	149.243	146	-2.2%	148	-0.8%	145	-2.8%
(IgG1)$_1$:(sEGFR)$_1$	*(236.7)*	241	1.8%	231	-2.4%	-	-
(IgG1)$_1$:(sEGFR)$_2$	*(324.2)*	327	0.9%	320	-1.3%	318	-1.9%
IgG1-RGY	149.607			148	-1.1%	160	6.9%
(IgG1-RGY)$_6$	897.645			965	7.5%	818	-8.9%
(sEGFR)$_{12}$:(IgG1-RGY)$_6$	*(1,947.6)*	1,942	-0.3%	1,929	-1.0%	1621	-16.8%
C1q	463.561			470	1.4%	444	-4.2%
(IgG1-RGY)$_6$:(A$_4$B$_4$C$_4$)	1,206.181			-	-	-	-
(IgG1-RGY)$_6$:C1q	1,361.042			1,425	4.7%	1252	-8.0%
(sEGFR)$_{12}$:(IgG1-RGY)$_6$:C1q	*(2,411.2)*	2,422	0.4%	2,354	-2.4%	1944	-19.4%

Table S2. MP-derived kinetic rates and equilibrium constants for IgG4Δhinge variants. Dissociation rates for IgG4Δhinge variants were determined by following the fractional occupancy over time for jump diluted high-concentration samples. A dilution series of each mutant was recorded and corrected for dissociation upon jump dilution using the determined k_{off} values. This enabled us to estimate the fractional occupancy in the original samples and to determine the K_d of the interaction. The k_{on} was subsequently calculated by dividing the k_{off} by the K_d. In the last column the values determined by native MS as previously reported by Rose et al.[1] are given.

IgG4Δhinge variant	k_{off} (s^{-1})	k_{on} (M^{-1} s^{-1})	K_d (M)	$K_{d,\ native\ MS}$ (M)[1]
R409K	$4.4 \cdot 10^{-5}$	$4.7 \cdot 10^{6}$	$9.4 \cdot 10^{-12}$	$4.0 \cdot 10^{-10}$
Wild-type	$9.2 \cdot 10^{-4}$	$3.1 \cdot 10^{5}$	$2.9 \cdot 10^{-9}$	$5.0 \cdot 10^{-8}$
D399S	$1.8 \cdot 10^{-2}$	$2.3 \cdot 10^{3}$	$7.8 \cdot 10^{-6}$	$4.4 \cdot 10^{-6}$
L368A	$3.0 \cdot 10^{-2}$	$5.5 \cdot 10^{2}$	$5.4 \cdot 10^{-5}$	$7.6 \cdot 10^{-6}$

Table S3. Advantages and disadvantages of MP, native MS and SEC-MALS in the analysis of antibodies and heavily glycosylated macromolecular immune complexes.

	Advantages	Disadvantages
MP	- Fastest - Most native conditions - Low sample consumption - Requires little training - Accurate quantification at nM range protein concentrations	- Limited mass resolution and accuracy - Not useful for interactions causing a small mass shift - Mass artifacts for some proteins - Limited to strongly bound and stable interactions at nM concentrations - Large excesses of certain components complicate the concomitant detection of particles at lower abundance - Available methodologies less robust in dilution and sample handling
Native MS	- Supreme mass resolution and accuracy - Accurate quantification at μM range protein concentrations - Workflows available for automated sample handling and high-throughput data collection	- Requires training - Requires buffer exchange - Hampered by extensive sample microheterogeneity - ESI process may induce dissociation for some protein complexes
Charge detection native MS	- Low sample consumption - Supreme mass resolution and accuracy also for highly heterogenous samples	- Requires extensive training - Not well established yet
SEC-MALS	- Non-destructive - Reliable quantification of protein abundance - Well-established for one-component systems and simple protein complexes - Highly robust workflows available for automated sample handling and high-throughput data collection	- Low resolution and mass accuracy - Not useful for interactions causing a small mass shift - Limited to slowly dissociating interactions - Highest sample consumption

Supplementary References

1.   Rose, Rebecca J.; Labrijn, Aran F.; van den Bremer, Ewald T. J.; Loverix, S.; Lasters, I.; van Berkel, Patrick H. C.; van de Winkel, Jan G. J.; Schuurman, J.; Parren, Paul W. H. I.; Heck, Albert J. R., Quantitative Analysis of the Interaction Strength and Dynamics of Human IgG4 Half Molecules by Native Mass Spectrometry. *Structure* **2011,** *19* (9), 1274-1282.

2.   Bleeker, W. K.; Lammerts van Bueren, J. J.; van Ojik, H. H.; Gerritsen, A. F.; Pluyter, M.; Houtkamp, M.; Halk, E.; Goldstein, J.; Schuurman, J.; van Dijk, M. A.; van de Winkel, J. G. J.; Parren, P. W. H. I., Dual Mode of Action of a Human Anti-Epidermal Growth Factor Receptor Monoclonal Antibody for Cancer Therapy. *J. Immunol.* **2004,** *173* (7), 4699-4707.

3.   de Jong, R. N.; Beurskens, F. J.; Verploegen, S.; Strumane, K.; van Kampen, M. D.; Voorhorst, M.; Horstman, W.; Engelberts, P. J.; Oostindie, S. C.; Wang, G.; Heck, A. J. R.; Schuurman, J.; Parren, P. W. H. I., A Novel Platform for the Potentiation of Therapeutic Antibodies Based on Antigen-Dependent Formation of IgG Hexamers at the Cell Surface. *PLoS Biol.* **2016,** *14* (1), e1002344.

4.   Wang, G.; de Jong, R. N.; van den Bremer, E. T.; Beurskens, F. J.; Labrijn, A. F.; Ugurlar, D.; Gros, P.; Schuurman, J.; Parren, P. W.; Heck, A. J., Molecular Basis of Assembly and Activation of Complement Component C1 in Complex with Immunoglobulin G1 and Antigen. *Mol. Cell* **2016,** *63* (1), 135-45.

5.   Wang, G.; Johnson, A. J.; Kaltashov, I. A., Evaluation of Electrospray Ionization Mass Spectrometry as a Tool for Characterization of Small Soluble Protein Aggregates. *Anal. Chem.* **2012,** *84* (3), 1718-1724.

6.   Marty, M. T.; Baldwin, A. J.; Marklund, E. G.; Hochberg, G. K. A.; Benesch, J. L. P.; Robinson, C. V., Bayesian Deconvolution of Mass and Ion Mobility Spectra: From Binary Interactions to Polydisperse Ensembles. *Anal. Chem.* **2015,** *87* (8), 4370-4376.

7.   Wörner, T. P.; Snijder, J.; Bennett, A.; Agbandje-McKenna, M.; Makarov, A. A.; Heck, A. J. R., Resolving heterogeneous macromolecular assemblies by Orbitrap-based single-particle charge detection mass spectrometry. *Nat Methods* **2020,** *17* (4), 395-398.

8.   Hastie, K.; Rayaprolu, V.; Saphire, E. O., Analysis of Oligomeric and Glycosylated Proteins by Size-Exclusion Chromatography Coupled with Multiangle Light Scattering. In *Mass Spectrometry of Glycoproteins: Methods and Protocols*, Delobel, A., Ed. Springer US: New York, NY, 2021; pp 343-359.

9.   Wang, G.; de Jong, R. N.; van den Bremer, E. T. J.; Parren, P. W. H. I.; Heck, A. J. R., Enhancing Accuracy in Molecular Weight Determination of Highly Heterogeneously Glycosylated Proteins by Native Tandem Mass Spectrometry. *Anal. Chem.* **2017,** *89* (9), 4793-4797.